Available online at www.sciencedirect.com
SCIENCE DIRECT®
Tetrahedron
Tetrahedron 60 (2004) 3251–3259

Self-assembly of β-turn forming synthetic tripeptides into supramolecular β-sheets and amyloid-like fibrils in the solid state

Samir Kumar Maji,[a] Debasish Haldar,[a] Michael G. B. Drew,[b] Arijit Banerjee,[a] Apurba Kumar Das[a] and Arindam Banerjee[a,*]

[a]*Department of Biological Chemistry, Indian Association for the Cultivation of Science, Jadavpur, Kolkata 700 032, India*
[b]*Department of Chemistry, The University of Reading, Whiteknights, Reading RG6 6AD, UK*

Received 19 November 2003; revised 12 January 2004; accepted 5 February 2004

Abstract—We have described here the self-assembling properties of the synthetic tripeptides Boc-Ala(1)-Aib(2)-Val(3)-OMe **1**, Boc-Ala(1)-Aib(2)-Ile(3)-OMe **2** and Boc-Ala(1)-Gly(2)-Val(3)-OMe **3** (Aib=α-amino isobutyric acid, β-Ala=β-alanine) which have distorted β-turn conformations in their respective crystals. These turn-forming tripeptides self-assemble to form supramolecular β-sheet structures through intermolecular hydrogen bonding and other noncovalent interactions. The scanning electron micrographs of these peptides revealed that these compounds form amyloid-like fibrils, the causative factor for many neurodegenerative diseases including Alzheimer's disease, Huntington's disease and Prion-related encephalopathies.

1. Introduction

Oligopeptides with appropriate conformations can self-assemble to form many regular structures such as sheets, ribbons, rods and tubes which have numerous applications in biological and material sciences.[1,2] For example, Ghadiri and his coworkers have established that self-assembling cyclic peptides form hollow nanotubes, which can act as artificial ion channels and biosensors.[3] Zhang and his colleagues have shown that a self-assembling peptide scaffold can serve as a substrate for neurite outgrowth and synapse formation and this type of biologically compatible scaffold is also important for tissue repair and tissue engineering.[4] Self-assembling peptides sometimes form gels when they encapsulate solvent molecules under suitable conditions.[5] Very recently, Artzner and his co-workers have demonstrated that self-assembly of a synthetic therapeutic octapeptide, Lanreotide, leads to the formation of supramolecular β-sheets which upon further self-assembly ultimately form monodisperse nanotubes in water with diameters that are tunable by suitable modifications in the molecular structure.[6] Higher order molecular self-assembly of a peptide into a β-sheet structure is not only important for designing biomaterials, but also useful in studying pathogenesis of certain age-related disease causing fibrils where self-assembly of mis-folded proteins or protein fragments leads to the formation of the aggregated mass that is known as amyloid fibrils.[7] The supramolecular β-sheet stabilization and consequent insoluble amyloid plaque formation are associated with several neurodegenerative diseases including Alzheimer's disease[8] and Prion-protein diseases.[9] Sequences and three dimensional structures of disease-causing amyloid proteins and/or protein fragments are enormously varied. However, they self-assemble into supramolecular β-sheets and consequently form protease resistant amyloid fibrils and exhibit similar physicochemical properties (viz.: congophilicity, binds to thioflavin T).[10] The therapeutic challenge in all forms of these fatal neurodegenerative diseases is to prevent amyloid fibril formation, a goal that requires a detailed understanding of the pathway(s) of β-sheet aggregation as well as fibrillation. Recently, many research groups also have used self-assembling, β-sheet forming peptides as amyloid fibril inhibitors.[11]

Previously, we have demonstrated that short peptides with extended backbone conformations can self-assemble to form supramolecular β-sheet structures in crystals and amyloid-like fibrils in the solid state.[12] As Aβ-peptides (Amyloid β-peptide) contain many short loops and turn conformations in their backbones,[13] self-assembly of turn-forming peptides is important for model studies. Recently, Kirschner and his co-workers measured the powder diffraction patterns of a solubilized and dried Aβ31-35 sample and demonstrated that this peptide adopts an intramolecular hydrogen bonded reverse-turn conformation which is important for amyloid fibril formation and its cytotoxicity.[14] However, the crystal structures of model peptides which form an intermolecularly hydrogen-bonded

Keywords: Amyloid-like fibril; β-Turn; Supramolecular β-sheet; Self-assembling peptides.
* Corresponding author. Tel.: +91-33-2473-4971; fax: +91-33-2473-2805; e-mail address: bcab@mahendra.iacs.res.in

0040–4020/$ - see front matter © 2004 Elsevier Ltd. All rights reserved.
doi:10.1016/j.tet.2004.02.019

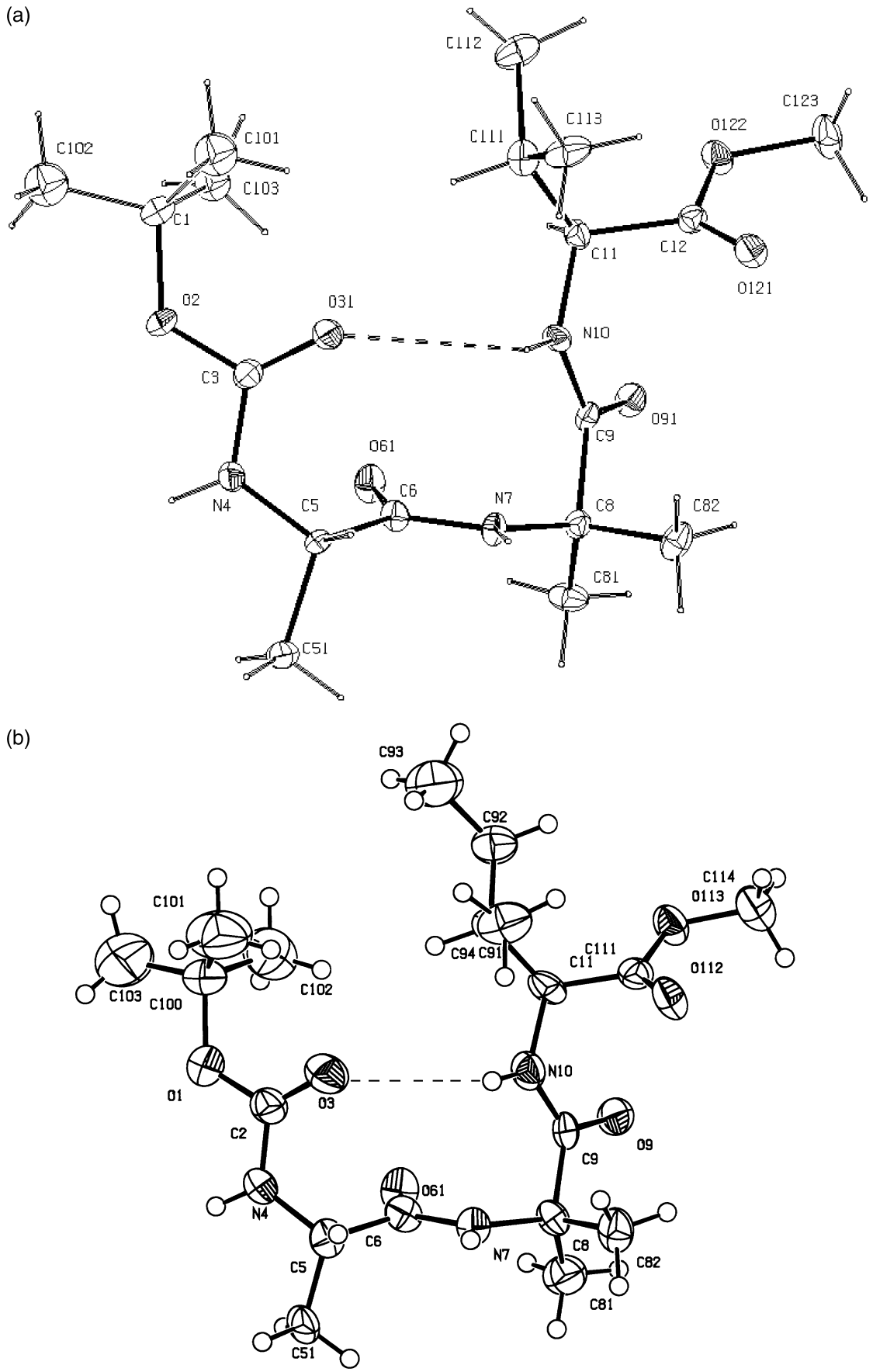

Figure 1 (*legend opposite*)

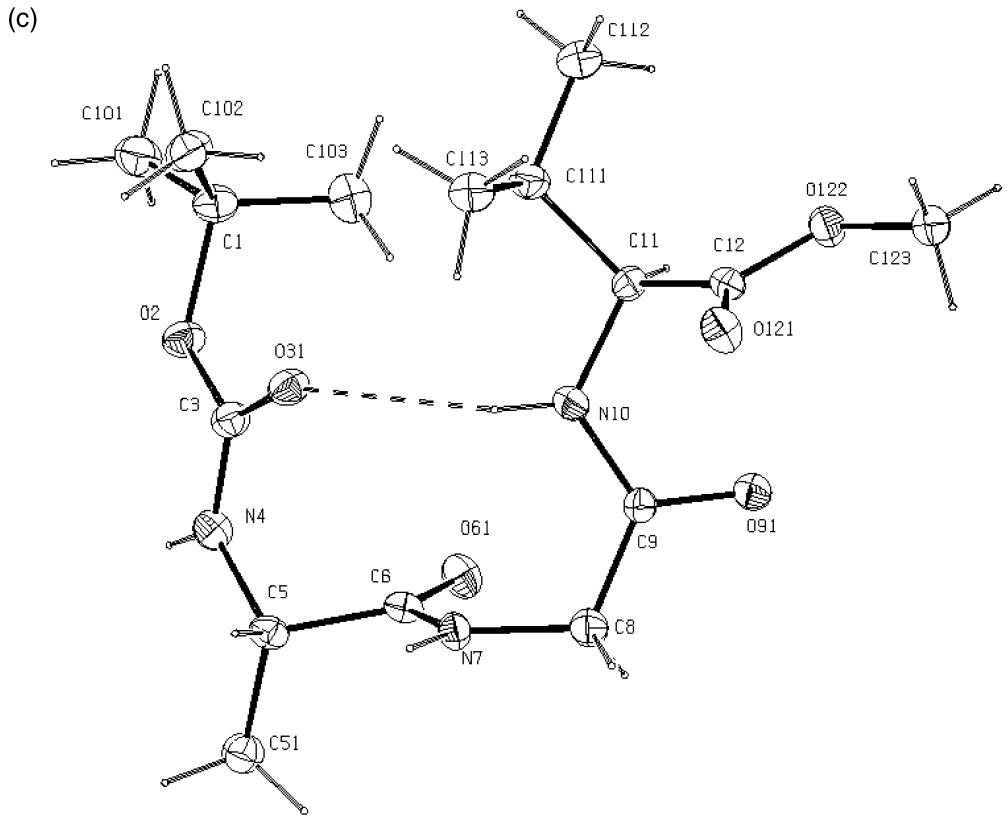

Figure 1. (a) The structure of peptide **1** showing the atomic numbering scheme. Ellipsoids at 20% probability. The weak intramolecular hydrogen bond is shown as a dotted line. (b) Molecular conformation of peptide **2** showing the atomic numbering scheme. The weak intramolecular hydrogen bond is shown as a dotted line. Ellipsoids at 30% probability. (c) ORTEP diagram with atomic numbering scheme of the peptide **3**. Thermal ellipsoids are shown at 30% probability level. The weak intramolecular hydrogen bond is shown as a dotted line.

supramolecular β-sheet from a turn-forming semi-cyclic peptide backbone are still rarely obtained. In our very recent communication, we have demonstrated that a β-turn forming peptide can form supramolecular β-sheet structure through self-aggregation and can exhibit amyloid-like fibrillar morphology in the solid state.[15] Continuing our research in this field, we report here the results of our studies on three synthetic terminally blocked tripeptides, Boc-Ala(1)-Aib(2)-Val(3)-OMe **1**, Boc-Ala(1)-Aib(2)-Ile(3)-OMe **2** and Boc-Ala(1)-Gly(2)-Val(3)-OMe **3** which all adopt reverse turn conformations and self-assemble to form supramolecular β-sheets in crystals and amyloid-like fibrils in the solid state.

2. Results and discussion

Peptides **1** and **2** contain the centrally located conformationally constrained Aib (α-aminoisobutyric acid) residue together with hydrophobic Val (valine) and Ile (isoleucine) residues at the C terminus and both adopt a turn structure. In tripeptide **3**, the centrally positioned Aib has been substituted by the structurally very flexible Gly (glycine) residue with the aim of investigating whether or not peptide **3** forms the folded turn conformation. These peptides were studied using X-ray crystallography, NMR, scanning electron microscopy and optical microscopy.

Table 1. Selected backbone torsion angles (°) of peptides **1**, **2** and **3**

Torsional angles	Peptide **1**	Peptide **2**	Peptide **3**
ω_0	169.6(7)	170.8(4)	173.9(6)
ϕ_1	−58.1(9)	−54.6(6)	−55.6(9)
ψ_1	146.7(6)	147.1(4)	139.6(6)
ω_1	170.6(6)	171.4(5)	171.0(6)
ϕ_2	60.1(9)	60.0(6)	72.7(8)
ψ_2	30.8(9)	30.0(5)	19.1(10)
ω_2	170.8(6)	170.6(4)	175.9(6)
ϕ_3	−63.8(8)	−60.8(5)	−56.7(8)
ψ_3	143.7(7)	142.2(4)	137.9(8)

Table 2. Intra and intermolecular hydrogen bonding parameters of peptides **1**, **2** and **3**

D-H···A	H···A (Å)	D···A (Å)	D-H···A (°)
Peptide **1**			
N10-H10···O31	2.89	3.61	142
N4–H4···O121[a]	2.33	3.10	150
N7–H7···O91[b]	2.14	3.00	172
Peptide **2**			
N10–H10···O3	2.77	3.48	141
N4–H4···O112[c]	2.37	3.12	145
N7–H7···O9[d]	2.16	3.02	172
Peptide **3**			
N10–H10···O31	2.56	3.29	143
N4–H4···O91[e]	2.29	3.03	145
N7–H7···O91[f]	2.10	2.93	160

[a] Symmetry equivalent $x+0.5$, $y+0.5$, z.
[b] Symmetry equivalent x, $1+y$, z.
[c] Symmetry equivalent $0.5+x$, $0.5+y$, z.
[d] Symmetry equivalent x, $1+y$, z.
[e] Symmetry equivalent $1-x$, $y-0.5$, $2-z$.
[f] Symmetry equivalent $x-1$, y, z.

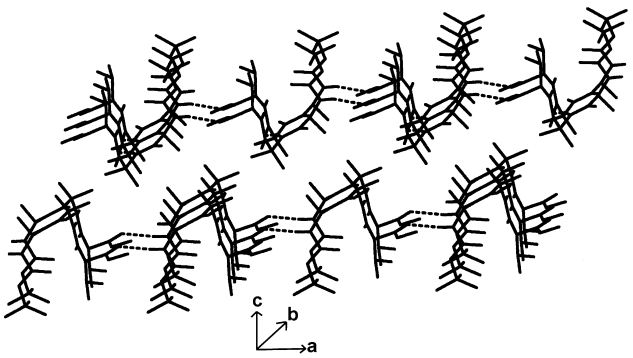

Figure 2. Packing of β-turn conformations of peptide **1** along the crystallographic *b* axis forming semi-cylindrical ribbon structure and further self-assembly along the crystallographic *a* and *b* axes to form a two dimensional monolayer β-sheet structure. Hierarchical self-assembly of individual β-sheets along the *c* direction results in the formation of a highly ordered cross β-sheet structure.

2.1. X-ray crystallography

The molecular conformations of tripeptides Boc-Ala(1)-Aib(2)-Val(3)-OMe **1**, Boc-Ala(1)-Aib(2)-Ile(3)-OMe **2** and Boc-Ala(1)-Gly(2)-Val(3)-OMe **3** are shown in Figure 1(a)–(c), respectively. Figure 1 reveals that peptides **1**, **2** and **3** adopt folded conformations corresponding to the distorted β-turn structure. Backbone torsion angles for these peptides **1**, **2** and **3** are listed in Table 1. For peptides **1** and **3** there exists a very weak 4⟶1 hydrogen bond between Boc-CO and Val (3) NH (N10···O31, 3.61 and 3.29 Å for **1** and **3**, respectively) and for peptide **2** the weak hydrogen bond is between Boc-CO and Ile(3) NH (N10···O3, 3.48 Å). These hydrogen bonds are illustrated in Figure 1(a)–(c) and dimensions are detailed in Table 2. In peptide **1** there are two intermolecular hydrogen bonds (N7–H7···O91 and N4–H4···O121) that are responsible for connecting individual peptide molecules to form and stabilize the

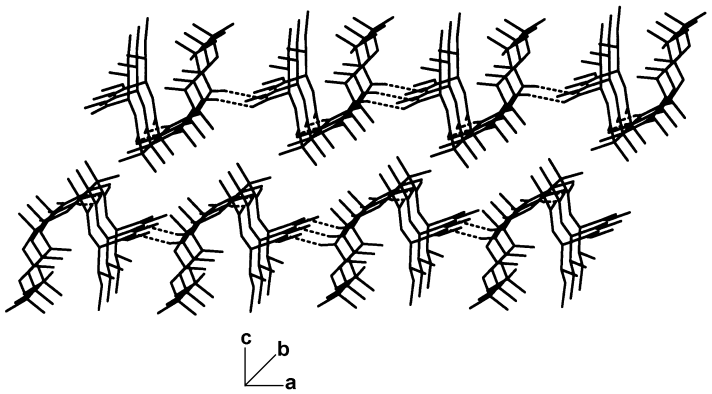

Figure 3. Two dimensional monolayer β-sheet structure obtained by the packing of individual β-turn conformations of peptide **2** along the crystallographic *a* and *b* axes which on further self-assembly gives supramolecular cross β-sheet structure along the *c* direction.

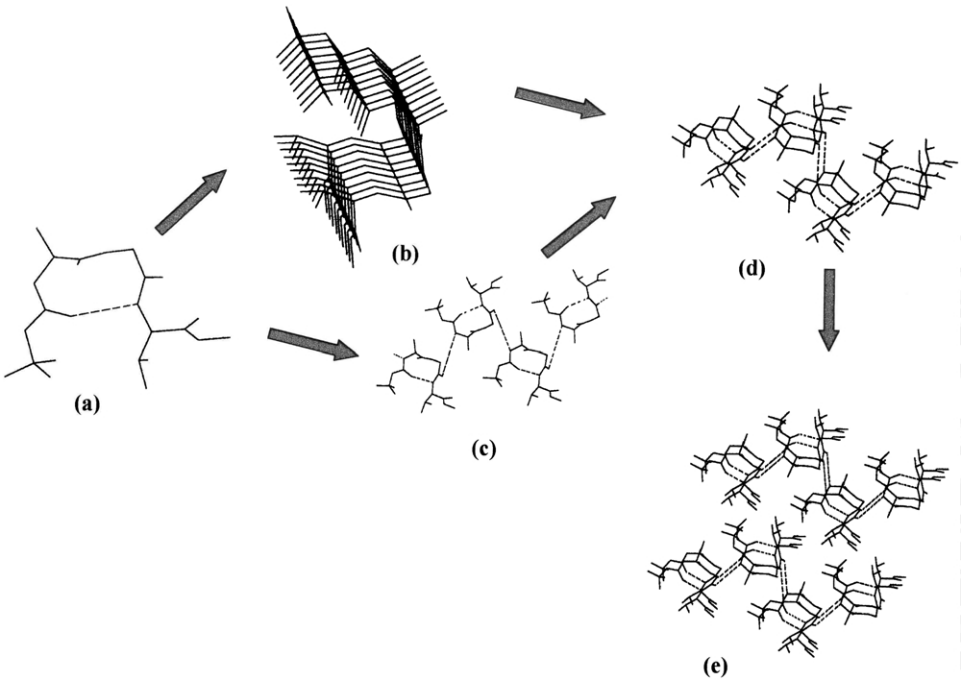

Figure 4. Self-assembly of peptide **3** in the β-turn conformation to form supramolecular β-sheet structure in crystal. (a) the β-turn building block, (b) packing of β-turn conformations along the crystallographic *a* axis forming semi-cylindrical ribbon structure, (c) and (d) the spacing of β-turn conformation along crystallographic *b* axis through intermolecular hydrogen bonds to form corrugated sheet like structures, (e) packing of individual β-sheets along the crystallographic *c* axis by van der Waals interactions forming highly ordered β-sheet structure in crystal.

Table 3. Crystal and data collection parameters of peptides **1**, **2** and **3**

	Peptide **1**	Peptide **2**	Peptide **3**
Empirical formula	$C_{18}H_{33}N_3O_6$	$C_{19}H_{35}N_3O_6$	$C_{16}H_{29}N_3O_6$
Crystallizing solvent	Dimethylsulphoxide	Methanol–water	Ethyl acetate
Crystal system	Monoclinic	Monoclinic	Monoclinic
Space group	*C*2	*C*2	$P2_1$
a(Å)	19.349(25)	19.345(22)	6.112(12)
b(Å)	6.094(10)	6.068(8)	12.515(14)
c(Å)	19.438(25)	20.323(21)	13.357(14)
α(°)	(90)	(90)	(90)
β(°)	101.34(1)	101.27(1)	102.89(1)
γ(°)	(90)	(90)	(90)
U(Å^3)	2248	2339	997
Z	4	4	2
Mol. wt.	387.5	401.5	359.4
Density (calcd, Mg/mm^3)	1.145	1.140	1.197
Unique data	3758	4115	3152
Observed reflns. ($I>2\sigma$ (I))	2347	2132	1246
R	0.1059	0.0736	0.0858
*wR*2	0.2440	0.1776	0.2554

supramolecular monolayer sheet assembly along the crystallographic *b* and *a* axes, respectively. These β-sheets are regularly stacked via van der Waals interactions as shown by the projection of the unit cells in the *c* direction to form the complex quaternary sheet structure (Fig. 2). The hydrogen bonding parameters of peptide **1** are listed in Table 2. In peptide **2**, the β-turn building blocks are aggregated via two unique intermolecular hydrogen bonds N7–H7···O9 and N4–H4···O112 (Table 2) along the *b* and *a* axes respectively to form two-dimensional sheet-like structures which on further self-assembly form a supramolecular β-sheet structure via van der Waals interactions in the *c* direction (Fig. 3). Figure 4 schematically illustrates the stepwise β-sheet formation for peptide **3**. Each turn-like conformation (Fig. 4(a)) self-assembles via an intermolecular hydrogen bond (N7–H7···O91) to form a semi-cylindrical ribbon structure along the short crystallographic *a* axis (Fig. 4(b)). These ribbons are connected along the screw axis parallel to *b* via intermolecular hydrogen bonds N4–H4···O91 to form two-dimensional corrugated sheet-like structures (Fig. 4(c)) which are regularly stacked via van der Waals interactions as shown by the projection of the unit cells in the *c* direction to form a supramolecular β-sheet structure (Fig. 4(e)). Hydrogen bonding data for peptide **3** are also listed in Table 2. Crystal data for these three peptides are detailed in Table 3.

Figure 5. SEM image of peptide **1** showing a bunch of rod-like fibrils in the solid state.

2.2. Morphology of peptides

The scanning electron microscope (SEM) was used for the morphological studies of these peptides. The SEM image of peptide **1** obtained from dried fibrous materials (which were grown slowly from methanol–water mixture) clearly shows that the aggregate in the solid state is a bundle of long filaments (Fig. 5). The SEM images (Figs. 6 and 7) of the dried fibrous materials (which were grown slowly from a methanol–water mixture) of peptides **2** and **3** exhibit that the aggregates in the solid state have amyloid-like fibrillar morphology.[16] Moreover, the time-dependent optical microscopic studies of peptide **1** in chloroform solution clearly indicates that these fibrils were grown from

Figure 6. Typical SEM image of peptide **2** in the solid state.

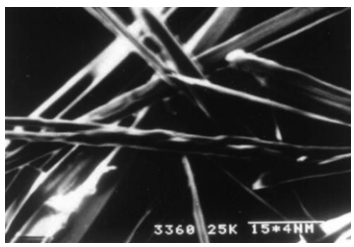

Figure 7. SEM image of peptide **3** exhibits filamentous fibrillar morphology in solid state.

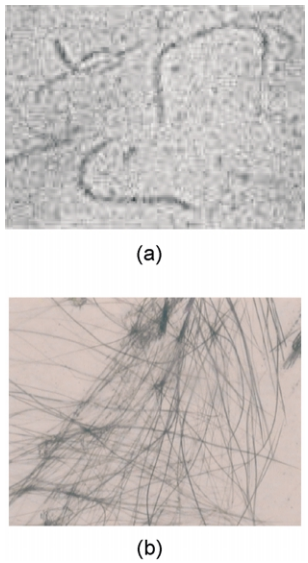

Figure 8. (a) Optical microscopic image of peptide **1** showing intermediate protofibril formation in $CHCl_3$ solution. (b) Optical microscopic image of peptide **1** showing full-length fibril formation in $CHCl_3$ solution.

relatively smaller protofibrils (Fig. 8(a)), which ultimately form higher order mature fibrils (Fig. 8(b)), a characteristic feature of amyloid fibril formation.[7b,d,17] These fibrils obtained from peptides **1**, **2** and **3** were stained with a physiological dye, Congo red, and exhibit distinct green-gold birefringence under polarized light (Fig. 9). These results are consistent with Congo red binding to an amyloid β-sheet fibrillar structure.[10]

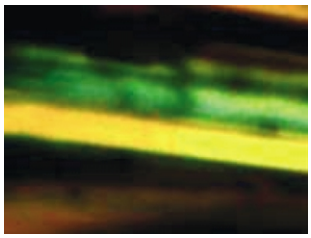

Figure 9. Congo red stained peptide **3** fibrils observed through crossed polarizers showing green-gold birefringence a characteristic feature of amyloid fibrils.

3. Conclusion

In spite of having different sequences and compositions, all three reported peptides adopt a distorted β-turn conformation in their crystal structures. Moreover, these turn-forming peptides self-associate to form supramolecular β-sheet structures via non-covalent interactions including intermolecular hydrogen bonds, in which all the hydrogen bonds are formed between the peptide linkages. These turn-forming peptides also form amyloid-like fibrils upon further self-aggregation, as is evident from the characteristic Congo red binding studies and observing the typical birefringence of these fibrils under a cross polarizer. So, these peptides represent a good model system for self-assembling β-sheets from turn-forming model synthetic peptides. These results have also established that the unconventional folded, β-turn-like structure (apart form the conventional extended backbone conformations) is a competent subunit for supramolecular β-sheets and amyloid-like fibrils in short model peptides.

4. Experimental

4.1. Peptide synthesis

The tripeptides were synthesized by conventional solution phase methods using racemization-free fragment condensation strategy.[18] The Boc group was used for N-terminal protection and the C terminus was protected as a methyl ester. Couplings were mediated by dicyclohexylcarbodiimide-1-hydroxybenzotriazole (DCC/HOBt). All intermediates have been characterized by ^1H NMR (300 MHz) and thin layer chromatography (TLC) on silica gel and used without further purification. The final products were purified by column chromatography using silica (100–200-mesh size) gel as stationary phase and ethyl acetate as eluent. Purified final compounds have been fully characterized by 300 MHz ^1H NMR spectroscopy.

4.1.1. Boc-Ala-OH (4). A solution of Ala (3.56 g, 40 mmol) in a mixture of dioxan (80 mL), water (40 mL) and 1 M NaOH (40 mL) was stirred and cooled in an ice-water bath. Di-*tert*-butylpyrocarbonate (9.6 g, 44 mmol) was added and stirring was continued at room temperature for 6 h. Then the solution was concentrated in vacuum to about 40–60 mL, cooled in an ice water bath, covered with a layer of ethyl-acetate (about 50 mL) and acidified with a dilute solution of $KHSO_4$ to pH 2–3 (congo red). The aqueous phase was extracted with ethyl acetate and this operation was done repeatedly. The ethyl acetate extracts were pooled, washed with water and dried over anhydrous Na_2SO_4 and evaporated in vacuum. Pure material was obtained as white solid.

Yield=7.308 g (36 mmol, 90%). Mp 85 °C. Anal. Calcd for $C_8H_{15}NO_4$ (189): C, 50.79; H, 7.94; N, 7.40. Found: C, 50.62; H, 7.77; N, 7.52.

4.1.2. Boc-Ala(1)-Aib(2)-OMe (5). A sample of Boc-Ala-OH (4.54 g, 24 mmol) was dissolved in dichloromethane (DCM) (40 mL) in an ice-water bath. H-Aib-OMe was isolated from the corresponding methyl ester hydrochloride (3.36 g, 48 mmol) by neutralization and subsequent extraction with ethyl acetate and the ethyl acetate extract was concentrated to 20 mL. This was added to the reaction mixture, followed immediately by di-cyclohexylcarbodiimide (DCC) (4.94 g, 24 mmol). The reaction mixture was allowed to come to room temperature and stirred for 24 h. DCM was evaporated, and the residue was taken up in ethyl acetate (30 mL), and dicyclohexylurea (DCU) was filtered off. The organic layer was washed with 2 M HCl (3×30 mL), brine, 1 M sodium carbonate (3×30 mL) and brine (2×30 mL) and dried over anhydrous sodium sulfate, and evaporated in vacuum to yield **5** as waxy solid.

Yield=5.48 g (19 mmol, 79.17 %). ^1H NMR ($CDCl_3$, 300 MHz, δ ppm): 6.77 [Aib(2)NH, 1H, s]; 5.06 [Ala(1) NH, 1H, d]; 4.16 [$C^{\alpha}Hs$ of Ala(1), 1H, t]; 3.73 [$-OCH_3$, 3H, s]; 1.54 [$C^{\beta}H_3$ s of Aib, 6H, s]; 1.45 [Boc-CH_3 s, 9H, s]; 1.35 [$C^{\beta}Hs$ of Ala(1), 3H, m]. Anal. Calcd for $C_{13}H_{24}N_2O_5$

(288): C, 54.16; N, 9.72; H, 8.33. Found: C, 54.4; N, 9.8; H, 8.5.

4.1.3. Boc-Ala(1)-Aib(2)-OH (6). To a sample of **5** (4.6 g, 16 mmol), MeOH (40 mL) and 2 M NaOH (24 mL) were added and the progress of saponification was monitored by thin layer chromatography (TLC). The reaction mixture was stirred. After 10 h, methanol was removed under vacuum, the residue was taken up in 30 mL of water, washed with diethyl ether (2×20 mL). Then the pH of the aqueous layer was adjusted to **2** using 1 M HCl and it was extracted with ethyl acetate (3×20 mL). The extracts were pooled, dried over anhydrous sodium sulfate, and evaporated in vacuum to yield 2.72 g of **6** as white solid.

Yield=2.72 g (13.6 mmol, 85%). Mp 176 °C. ^{1}H NMR ($(CD_3)_2SO$, 300 MHz, δ in ppm): 11.8 [–COOH, 1H, br.]; 7.8 [Aib(2) NH, 1H, s]; 6.73 [Ala(1) NH, 1H, d]; 3.94 [C$^\alpha$Hs of Ala(1), 1H, m]; 1.41 [C$^\beta$H$_3$ s of Aib(2), 6H, s]; 1.36 [Boc-CH$_3$ s, 9H, s]; 1.14 [C$^\beta$H$_3$ s of Ala(1), 3H, m]. Anal. Calcd for $C_{12}H_{22}N_2O_5$ (274): C, 52.55; N, 10.21; H, 8.029. Found: C, 52.6; N, 10.16; H, 8.2.

4.1.4. Boc-Ala(1)-Aib(1)-Val(3)-OMe 1. A sample of Boc-Ala-Aib-OH (0.82 g, 3 mmol) in DMF (8 mL) was cooled in an ice-water bath and H-Val-OMe was isolated from the corresponding methyl ester hydrochloride (1.0 g, 6 mmol) by neutralization, subsequent extraction with ethyl acetate and concentration (5 mL) and it was added to the reaction mixture, followed immediately by DCC (0.62 g, 3 mmol) and HOBt (0.4 g, 3 mmol). The reaction mixture was stirred for 3 days. The residue was taken in ethyl acetate (20 mL) and the DCU was filtered off. The organic layer was washed with 2 M HCl (3×20 mL), brine, 1 M sodium carbonate (3×20 mL), brine (2×20 mL), dried over anhydrous sodium sulfate and evaporated in vacuum to yield 0.77 g (2 mmol, 66.66 %) of white solid. Purification was done by silica gel column (100–200 mesh) using ethyl acetate as eluent. Colourless single crystals were grown from dimethylsulphoxide by slow evaporation.

Yield=0.77 g (2 mmol, 66.66 %). Mp 184 °C. ^{1}H NMR ($CDCl_3$, 300 MHz, δ ppm): 7.06 [Val (3) NH, 1H, d, J= 4.58 Hz]; 6.71 [Aib(2) NH, 1H, s]; 4.96 [Ala(1) NH, 1H, d, J=4.98 Hz]; 4.50 [C$^\alpha$H of Ala(1), 1H, m]; 4.09 [C$^\alpha$H of Val(3), 1H, m]; 3.74 [–OCH$_3$, 3H, s]; 2.16–2.20 [C$^\beta$H of Val(3), 1H, m]; 1.54 [C$^\beta$Hs of Aib, 6H, s]; 1.45 [Boc-CH$_3$, 9H, s]; 1.35, 1.36 [C$^\beta$Hs of Ala(1), 3H, d, J=4.23 Hz]; 0.89–0.94 [C$^\gamma$Hs of Val (3), 6H, m]. Anal. Calcd for $C_{18}H_{33}N_3O_6$ (387): C, 55.81; H, 8.53; N, 10.85. Found: C, 55.75; H, 8.37; N, 11.92. Mass spectral data M+Na$^{+=}$410, M_{calcd}=387.

4.1.5. Boc-Ala(1)-Aib(2)-Ile(3)-OMe (2). Boc-Ala-Aib-OH (1.37 g, 5 mmol) in DMF (15 mL) was cooled in an ice-water bath and H-Ile-OMe was isolated from the corresponding methyl ester hydrochloride (1.82 g, 10 mmol) by neutralization and subsequent extraction with ethyl acetate and the ethyl acetate extract was concentrated to 8 mL. It was then added to the reaction mixture, followed immediately by DCC (1.03 g, 5 mmol) and HOBt (0.68 g, 5 mmol). The reaction mixture was stirred for 3 days. The residue was taken up in ethyl acetate 20 mL and the DCU was filtered off. The organic layer was washed with 2 M HCl (3×40 mL), brine, 1 M sodium carbonate (3×40 mL), brine (2×40 mL), dried over anhydrous sodium sulfate and evaporated in vacuum to yield 1.6 g (4 mmol) of white solid. Purification was done by silica gel column (100–200 mesh) using ethyl acetate as eluent.

Yield=1.6 g, 80%. Mp 178 °C. ^{1}H NMR ($CDCl_3$, 300 MHz, δ ppm): 7.08 [Ile(3) NH, 1H, d, J=8.16 Hz]; 6.68 [Aib(2) NH 1H, s]; 4.96 [Ala(1) NH,1H, d, J=7.5 Hz]; 4.51–4.55 [C$^\alpha$H of Ala(1), 1H, m]; 4.09–4.11 [C$^\alpha$H of Ile(3), 1H, m]; 3.72 [–OCH$_3$, 3H, s]; 1.89–1.94 [C$^\beta$Hs of Ile(3), 1H, m]; 1.61 [C$^\beta$H$_3$ s of Aib(2), 6H, s]; 1.45 [Boc-CH$_3$ s, 9H, s]; 1.34–1.39 [C$^\beta$Hs of Ala(1), 3H, d, J=8.82 Hz]; 1.25 [C$^\gamma$s of Ile(3), 3H, d]; 0.89–0.96 [C$^\gamma$s & C$^\delta$Hs of Ile(3), 5H, m]. Anal. Calcd for $C_{19}H_{35}N_3O_6$ (401): C, 56.85; N, 10.47; H, 8.72. Found: C, 56.71; N, 10.35; H, 8.8. Mass spectral data M+Na$^+$ +H$^+$=425, M_{calcd}=401.

4.1.6. Boc-Ala(1)-Gly(2)-OBz (7). A sample of Boc-Ala-OH (3.78 g, 20 mmol) was dissolved in a mixture of dichloromethane-*N*,*N*-dimethylformamide (DCM/DMF) (30 mL) in an ice-water bath. H-Gly-OCH$_2$Ph was isolated from of the corresponding benzyl ester *p*-toluene sulphonate (13.48 g, 40 mmol) by neutralization, subsequent extraction with ethyl acetate and concentration (10 mL) and this was added to the reaction mixture, followed immediately by di-cyclohexaylcarbodiimide (DCC) (4.12 g, 20 mmol) and 1-hydroxybenzotriazole (HOBt) (2.7 g, 20 mmol). The reaction mixture was allowed to come to room temperature and stirred for 24 h. DCM was evaporated, the residue was taken in ethyl acetate (40 mL), and dicyclohexylurea (DCU) was filtered off. The organic layer was washed with 2 M HCl (3×40 mL), brine, 1 M sodium carbonate (3×40 mL) and brine (2×40 mL) and dried over anhydrous sodium sulfate, and evaporated in vacuum to yield of the dipeptide **7** as white solid.

Yield=5.712 g (17 mmol, 85%). Mp 73 °C. ^{1}H NMR ($CDCl_3$, 300 MHz, δ ppm): 7.35 [Ph, 5H, m]; 6.73 [Gly(2) NH, 1H, t]; 5.18 [-benzyl CH$_2$, 2H, s]; 5.01–5.03 [Ala(1) NH, 1H, d]; 4.22 [C$^\alpha$H of Ala(1), 1H, t]; 4.04–4.09 [C$^\alpha$Hs of Gly(2), 2H, t]; 1.44 [Boc-CH$_3$, 9H, s]; 1.35–1.37 [C$^\beta$Hs of Ala(1), 3H, d]. Anal. Calcd for $C_{17}H_{24}N_2O_5$ (336): C, 60.71; H, 7.14; N, 8.33. Found: C, 60.67; H, 6.98; N, 8.36.

4.1.7. Boc-Ala(1)-Gly(2)-OH (8). To Boc-Ala(1)-Gly(2)-OBz **7** (4.37 g, (13 mmol), MeOH (40 mL) and 2 M NaOH (15 mL) were added and the progress of saponification was monitored by thin layer chromatography (TLC). The reaction mixture was stirred. After 10 h methanol was removed under vacuum, the residue was taken in 20 mL of water, washed with diethyl ether (2×20 mL). Then the pH of the aqueous layer was adjusted to **2** using 1 M HCl and it was extracted with ethyl acetate (3×20 mL). The extracts were pooled, dried over anhydrous sodium sulfate, and evaporated in vacuum to yield 2.70 g of **8** as white solid.

Yield=2.70 g (11 mmol, 84.61%). Mp 88 °C. ^{1}H NMR (70% $(CD_3)_2SO$+30% $CDCl_3$, 300 MHz, δ in ppm): 12.4 [–COOH, 1H, br]; 7.93 [Gly(2) NH, 1H, t]; 6.67 [Ala(1)

NH, 1H, d]; 4.06 [$C^{\alpha}H$ of Ala(1), 1H, t]; 3.76–3.80 [$C^{\alpha}Hs$ Gly(2), 2H, m]; 1.40 [Boc-CH_3, 9H, s];1.22–1.24 [$C^{\beta}Hs$ of Ala(1), 3H, m]. Anal. Calcd for $C_{10}H_{18}N_2O_5$ (246): C, 48.78; H, 7.31; N, 11.38. Found: C, 48.66; H, 7.29; N, 11.42.

4.1.8. Boc-Ala(1)-Gly(2)-Val(3)-OMe (3). A sample of Boc-Ala-Gly-OH (1.23 g, 5 mmol) in DMF (10 mL) was cooled in an ice-water bath and H-Val-OMe was isolated from the corresponding methyl ester hydrochloride (1.67 g, 10 mmol) by neutralization, subsequent extraction with ethyl acetate and concentration (7 mL) and it was added to the reaction mixture, followed immediately by of DCC (1.03 g, 5 mmol) and HOBt (0.67 g, 5 mmol). The reaction mixture was stirred for 3 days. The residue was taken in ethyl acetate (40 mL) and the DCU was filtered off. The organic layer was washed with 2 M HCl (3×40 mL), brine, 1 M sodium carbonate (3×40 mL), brine (2×40 mL), dried over anhydrous sodium sulfate and evaporated in vacuum to yield 1.32 g of white solid. Purification was done by silica gel column (100–200 mesh) using ethyl acetate as eluent. Colourless single crystals were grown from ethyl acetate by slow evaporation.

Yield=1.32 g (3.7 mmol, 74%). Mp 97 °C. ^1H NMR ($CDCl_3$, 300 MHz, δ ppm): 6.90 [Gly(2) NH, 1H, t]; 6.68 [Val (3) NH, 1H, d, J=8.4 Hz]; 5.02 [Ala(1) NH, 1H, d, J=6.6 Hz]; 4.52 [$C^{\alpha}H$ of Ala(1), 1H, m]; 4.23 [$C^{\alpha}H$ of Val(3), 1H, m]; 3.95–4.0 [$C^{\alpha}Hs$ of Gly(2), 2H, m]; 3.73 [$-OCH_3$, 3H, s]; 2.16–2.22 [$C^{\beta}H$ of Val(3), 1H, m]; 1.44 [Boc-CH_3, 9H, s]; 1.37–1.40 [$C^{\beta}Hs$ of Ala(1), 3H, d, J= 7.2 Hz]; 0.89–0.95 [$C^{\gamma}Hs$ of Val(3), 6H, m]. Mass spectral data $M+Na^{+}$=382, M_{calcd}=359. Anal. Calcd for $C_{16}H_{29}N_3O_6$ (359): C, 53.48; H, 8.07; N, 11.70. Found: C, 53.46; H, 8.02; N, 11.77.

4.2. Single crystal X-ray diffraction study

For tripeptides **1**, **2** and **3** intensity data were collected with Mo K_{α} radiation using the MAR research Image Plate System. For all peptides the crystals were positioned at 70 mm from the Image Plate. Selected details of the structure solutions and refinements are given in Table 3. 100 frames were measured at 2° intervals with a counting time of 2–5 min for various peptides. Data analyses were carried out with the XDS program.[19] The structures were solved using direct methods with the Shelx86[20] program. For peptide **1**, the *tert*-butyl group was disordered, with each methyl group taking up two different sites each refined with 50% occupancy. Apart from the disordered atoms in peptide **1**, all non-hydrogen atoms of all peptides were refined with anisotropic thermal parameters. The hydrogen atoms were included in geometric positions and given thermal parameters equivalent to 1.2 times those of the atom to which they were attached. The structures were refined on F^2 using Shelxl.[21] Crystallographic data for the three structures have been deposited at the Cambridge Crystallographic Data Center (CCDC 222157, 222158 and 173625).

4.3. NMR experiments

All NMR studies were carried out on a Brüker DPX 300 MHz spectrometer at 300 K. Peptide concentrations were in the range 1–10 mM in $CDCl_3$ and $(CD_3)_2SO$.

4.4. Mass spectrometry

Mass spectra of final compounds (tripeptides **1**, **2** and **3**) were recorded on a HEWLETT PACKARD Series 1100MSD mass spectrometer by positive mode electrospray ionization.

4.5. Morphological study

The Morphology of the tripeptides was investigated using an optical microscope and scanning electron microscope (SEM). For the SEM study, fibrous materials (slowly grown from methanol–water mixtures) were dried and gold coated. Then the micrographs were taken in a SEM apparatus (Hitachi S-415A). For the optical microscopic study of the peptide **1** in $CHCl_3$, Olympus CH 30 imaging microscope equipped with Image Pro Plus ver 4.0 software was used.

4.6. Congo red binding study

An alkaline saturated Congo red solution was prepared. The peptide fibrils were stained with alkaline Congo red solution (80% methanol/20% glass distilled water containing 10 μL of 1% NaOH) for 2 min then the excess stain (Congo red) was removed by rinsing the stained fibril with 80% methanol/20% glass distilled water solution for several times. The stained fibrils were dried in vacuum at room temperature for 24 h, then visualized at 100× or 500× magnification and birefringence was observed between crossed polarizers.

Acknowledgements

We thank EPSRC and the University of Reading, UK for funds for the Image Plate System. We also acknowledge Department of Science and Technology, New Delhi, India for the grant No. SR/S5/OC-29/2003.

References and notes

1. (a) Krejchi, M. T.; Atkins, E. D. T.; Waddon, A. J.; Fournier, M. J.; Mason, T. L.; Tirrell, D. A. *Science* **1994**, *265*, 1427–1432. (b) Aggeli, A.; Boden, N.; Cheng, Y.; Findlay, J. B. C.; Knowles, P. F.; Kovatchev, P.; Turnbull, P. J. H. *Biochemistry* **1996**, *35*, 16213–16221. (c) Otzen, D. E.; Kristensen, O.; Oliveberg, M. *Proc. Natl Acad. Sci. USA* **2000**, *97*, 9907–9912.
2. (a) Whetesides, G. M.; Mathias, J. P.; Seto, C. T. *Science* **1991**, *254*, 1312–1319. (b) Lehn, J. M. *Science* **1993**, *260*, 1762–1763. (c) Bong, D. T.; Clark, T. D.; Granja, J. R.; Ghadiri, M. R. *Angew. Chem., Int. Ed.* **2001**, *40*, 988–1011.
3. (a) Granja, J. R.; Ghadiri, M. R. *J. Am. Chem. Soc.* **1994**, *116*, 10785–10786. (b) Ghadiri, M. R.; Granja, J. R.; Milligran, R. A.; McRee, D. E.; Khazanovich, N. *Nature* **1993**, *366*, 324–327. (c) Ghadiri, M. R.; Granja, J. R.; Buehler, L. K. *Nature* **1994**, *369*, 301–304. (d) Hartgerink, J. D.; Clark, T. D.; Ghadiri, M. R. *Chem. Eur. J.* **1998**, *4*, 1367–1372. (e) Hartgerink, J. D.; Granja, J. R.; Milligan, R. A.; Ghadiri, M. R. *J. Am. Chem. Soc.* **1996**, *118*, 43–50.

4. Holmes, T. C.; Lacalle, S. D.; Su, X.; Liu, G.; Rich, A.; Zhang, S. *Proc. Natl Acad. Sci. USA* **2000**, *97*, 6728–6733.
5. (a) Aggeli, A.; Bell, M.; Boden, N.; Keen, J. N.; Knowles, P. F.; Mcleish, T. C. B.; Pitkeathly, M.; Radford, S. E. *Nature* **1997**, *386*, 259–262. (b) Maji, S. K.; Malik, S.; Drew, M. G. B.; Nandi, A. K.; Banerjee, A. *Tetrahedron Lett.* **2003**, *44*, 4103–4107.
6. Valéry, C.; Paternostre, M.; Robert, B.; Gulik-Krzywicki, T.; Narayanan, T.; Dedieu, J.; Keller, G.; Torres, M.; Cherif-Cheikh, R.; Calvo, P.; Artzner, F. *Proc. Natl Acad. Sci. USA* **2003**, *100*, 10258–10262.
7. (a) Koo, E. H.; Lansbury, Jr., P. T.; Kelly, J. W. *Proc. Natl Acad. Sci. USA* **1999**, *96*, 9989–9990. (b) Walsh, D. M.; Hartley, D. M.; Kusumoto, Y.; Fezoui, Y.; Condron, M. M.; Lomakin, A.; Benedek, G. B.; Selkoe, D. J.; Teplow, D. B. *J. Bio. Chem.* **1999**, *274*, 25945–25952. (c) Goldfarb, L. G.; Brown, P.; Haltia, M.; Ghiso, J.; Frangione, B.; Gajdusek, D. C. *Proc. Natl Acad. Sci. USA* **1993**, *90*, 4451–4454. (d) Walsh, D.; Lomakin, M. A.; Benedek, G. B.; Condron, M. M.; Teplow, D. B. *J. Bio. Chem.* **1997**, *272*, 22364–22372.
8. (a) Taubes, G. *Science* **1996**, *271*, 1493–1495. (b) Lansbury, Jr. P. T. *Acc. Chem. Res.* **1996**, *29*, 317–321. (c) Roses, A. D. *Curr. Opin. Neurobio.* **1996**, *644*, 650. (d) Baumeister, R.; Eimer, S. *Angew. Chem., Int. Ed.* **1998**, *37*, 2978–2982.
9. (a) Prusiner, S. B. *Proc. Natl Acad. Sci. USA* **1998**, *95*, 13363–13383. (b) Baldwin, M. A.; Cohen, F. E.; Prusiner, S. B. *J. Bio. Chem.* **1995**, *270*, 19197–19200. (c) Ng, S. B. L.; Doig, A. *J. Chem. Soc. Rev.* **1997**, *26*, 425–432.
10. (a) Kim, Y. S.; Randolph, T. W.; Manning, M. C.; Stevens, F. J.; Carpenter, J. F. *J. Bio. Chem.* **2003**, *278*, 10842–10850. (b) Taylor, D. L.; Allen, R. D.; Benditt, E. P. *J. Histochem. Cytochem.* **1974**, *22*, 1105–1112. (c) Lim, A.; Makhov, A. M.; Bond, J.; Tnouye, H.; Conmors, L. H.; Griffith, J. D.; Erickson, W. B.; Kirschner, D. A.; Costello, C. E. *J. Struct. Bio.* **2000**, *130*, 363–370. (d) Azriel, R.; Gazit, E. *J. Bio. Chem.* **2001**, *226*, 34156–34161.
11. Mason, J. M.; Kokkoni, N.; Stott, K.; Doig, A. J. *Curr. Opin. Struct. Bio.* **2003**, *13*, 1–7.
12. (a) Maji, S. K.; Drew, M. G. B.; Banerjee, A. *Chem. Commun.* **2001**, 1946–1947. (b) Banerjee, A.; Maji, S. K.; Drew, M. G. B.; Haldar, D.; Banerjee, A. *Tetrahedron Lett.* **2003**, *44*, 6741–6744. (c) Maji, S. K.; Haldar, D.; Banerjee, A.; Banerjee, A. *Tetrahedron* **2002**, *58*, 8695–8702. (d) Maji, S. K.; Haldar, D.; Velmurugan, D.; Rajakannan, V.; Banerjee, A. *Lett. Pept. Sci.* **2002**, *8*, 61–67.
13. Kirschner, D. A.; Inouye, H.; Bond, J. P.; Deverin, S. P.; Teeter, M. T.; El-Agnaf, O. M. A.; Henry, C.; Costello, C. E.; Lim, A. *Polym. Prepr.* **2002**, *43*, 187–188.
14. Bond, J. P.; Deverin, S. P.; Inouye, H.; EI-Agnaf, O. M. A.; Teeter, M. M.; Kirschner, D. A. *J. Struct. Bio.* **2003**, *41*, 156–170.
15. Banerjee, A.; Maji, S. K.; Drew, M. G. B.; Haldar, D.; Banerjee, A. *Tetrahedron Lett.* **2003**, *44*, 335–339.
16. (a) Sipe, J. D.; Cohen, A. S. *J. Struct. Bio.* **2000**, *130*, 88–98. (b) Goldsbury, C. S.; Wirtz, S.; Müller, S. A.; Sunderji, S.; Wicki, P.; Aebi, U.; Frey, P. *J. Struct. Bio.* **2000**, *130*, 217–231.
17. Nilsberth, C.; Westlind-Danielsson, A.; Eckman, C. B.; Condron, M. M.; Axelman, K.; Forsell, C.; Stenh, C.; Luthman, J.; Teplow, D. B.; Younkin, S. G.; Näslund, J.; Lannfelt, L. *Nat. Neurosci.* **2001**, *4*, 887–893.
18. Bodanszky, M.; Bodanszky, A. *The practice of peptide synthesis*. Springer: New York, 1984; pp 1–282.
19. Kabsch, W. *J. Appl. Cryst.* **1988**, *21*, 916.
20. Sheldrick, G. M. *Acta. Crystallogr. Sect. A: Fundam. Crystallogr.* **1990**, *46*, 467.
21. Sheldrick, G. M. *Program for Crystal Structure Refinement*; University of Göttingen: Germany, 1993.